

# Dispersive censor of acoustic spacetimes with a shock-wave singularity

Uwe R. Fischer<sup>✉</sup> and Satadal Datta<sup>✉</sup>

*Seoul National University, Department of Physics and Astronomy, Center for Theoretical Physics, Seoul 08826, Korea*

 (Received 9 September 2022; accepted 8 March 2023; published 12 April 2023)

A dispersionless shock wave in a fluid without friction develops an acoustic spacetime singularity which is naked (not hidden by a horizon). We show that this naked nondispersive shock-wave singularity is prohibited to form in a Bose-Einstein condensate, due to the microscopic structure of the underlying æther and the resulting effective trans-Planckian dispersion. Approaching the instant of shock  $t_{\text{shock}}$ , rapid spatial oscillations of density and velocity develop around the shock location, which begin to emerge already slightly before  $t_{\text{shock}}$ , due to the quantum pressure in the condensate. These oscillations render the acoustic spacetime structure completely regular, and therefore lead to a removal (censoring) of the spacetime singularity. Thus, distinct from the cosmic censorship hypothesis of Penrose formulated within Einsteinian gravity, the quantum pressure in Bose-Einstein condensates censors (prohibits) the formation of a naked shock-wave singularity, instead of hiding it behind a horizon.

DOI: [10.1103/PhysRevD.107.084023](https://doi.org/10.1103/PhysRevD.107.084023)

## I. INTRODUCTION

In Einsteinian gravity, singularities are ubiquitous [1–3]. However, the physical spacetime nature of these singularities is still under debate. The singularity theorems by Hawking and Penrose state that if there either exists a trapped surface due to gravitational collapse or the Universe is assumed to be spatially closed, spacetime singularities are formed with the following conditions being satisfied: We have Einstein gravity at zero or negative cosmological constant, the weak energy condition is maintained, closed timelike curves are absent, and every timelike or null geodesic enters a region where the curvature is not specially aligned with the geodesic [4–7]. As these theorems guarantee that if there exists a trapped surface in spacetime, a singularity must form, one may ask the question if the reverse holds true, and whether a singularity may form without a horizon enclosing it (naked singularity). The cosmic censorship hypothesis (CCH), then, in its weak form, states that generic gravitational collapse, starting from a nonsingular initial state, cannot create a naked singularity in spacetime [2,8,9].

However, explicit counterexamples to the CCH, for physically viable processes, have been found cf., e.g., [10–14]. On the other hand, mechanisms arguing that naked singularities are indeed hidden were developed, among which *backreaction* is a prominent example [15–18]. It is thus fair to say that the CCH is still widely debated, as regards the possible mechanisms for either violating or preserving it, and whether these mechanisms are of quantum or classical origin, also cf. Ref. [19]. This is largely due to the fact that there is no applicable quantum theory of gravity, in particular complete in the ultraviolet, with which

to ascertain whether a given argument for (or against) the CCH is true.

The seminal paper of Unruh [20] triggered, especially recently, with a substantial improvement of experimental capabilities, on a broad front a field which was coined analog gravity [21]. Its essence is that it models the propagation of classical and quantum fields on curved spacetime backgrounds, exploring various phenomena inaccessible at present in the realm of gravity proper, see, e.g., Refs. [22–39]. A particularly promising arena are Bose-Einstein condensates (BECs) due to the atomic precision control and accurate correlation function resolution they offer [40–61].

Acoustic black holes (“dumb” holes [62]) or cosmological horizons are thus well established and experimentally realized within the analog gravity realm. On the other hand, distinct from Einstein gravity, where singularities are ubiquitous, singularities in quantum fluids, and with particular regard to their acoustic spacetime properties, have not been much studied yet, to the best of our knowledge. It is important here to pause, and to clearly state at the outset the most important differences of analog gravity and Einstein gravity: In analog gravity, the acoustic spacetime metric is governed by nonlinear fluid dynamics and not by a solution of the Einstein equations. In Einstein gravity, black holes (and, as a result, also singularities in spacetime due to the theorems by Hawking and Penrose) are formed from gravitational collapse of matter. In fluids, it is the transition of subsonic to supersonic flow which creates an effective dumb hole horizon for linear sound in the medium. Distinct from Einstein gravity, this analog gravitational field, providing a background effective

spacetime for linear perturbations on top of it, is governed by a velocity scalar [63], in a comparable way to a nonlinear self-interacting scalar field theory of gravity [64]. In the present work, we establish a highly nonlinear process creating a naked singularity in the acoustic spacetime metric, physically represented by a shock wave in a BEC without dispersion included [that is in the so-called Thomas-Fermi (TF) limit]. For this nondispersive shock, the nonlinearity causes a stepwise discontinuity in the acoustic metric components, and as a result a naked timelike Ricci curvature singularity of the effective spacetime emerges.

In the real quantum fluid, dispersive effects can, however, not be neglected, due to the quantum pressure, which occurs because of the stiffness of the condensate order parameter (scalar field) against spatial variations of its modulus. We reveal as a result a dispersive censorship of the spacetime singularity, when a nondispersive shock wave [65] would develop a singularity of the effective spacetime at its front. Because of the dynamical differences of Einsteinian and analog gravity based on fluid-dynamical motion, here the singularity is censored (prohibited to form), instead of being dressed by a spacetime horizon. Our aim in the present investigation is thus to provide a realistic scenario, which can be experimentally implemented in a BEC, wherein the quantum pressure censors prohibits the formation of a singularity in an acoustic spacetime metric. We therefore demonstrate that the CCH, which asserts that the naked singularity is hidden behind a horizon, is in general not necessary, provided one admits alternative theories of gravity.

## II. FLUID DYNAMICS OF DILUTE BOSE-EINSTEIN CONDENSATES

### A. Fluid perturbations

Dilute BECs represent inviscid, barotropic, and irrotational fluids, where, importantly, the quantum pressure term is added to the Euler equation. Setting the atomic mass  $m = 1$ , we have to solve the following set [66]:

$$\partial_t \rho + \nabla \cdot (\rho \mathbf{v}) = 0, \quad (1)$$

$$\partial_t \mathbf{v} + \mathbf{v} \cdot \nabla \mathbf{v} = -\frac{\nabla p}{\rho} + \frac{\hbar^2}{2} \nabla \left( \frac{\nabla^2 \sqrt{\rho}}{\sqrt{\rho}} \right) - \nabla V_{\text{ext}}, \quad (2)$$

$$p = p(\rho) = \frac{1}{2} g \rho^2, \quad (3)$$

$$\nabla \times \mathbf{v} = 0 \quad \Rightarrow \quad \mathbf{v} = \nabla \Phi. \quad (4)$$

These equations are the only field equations occurring in our problem for condensate density  $\rho(\mathbf{r}, t)$  and condensate

velocity  $\mathbf{v}(\mathbf{r}, t)$ , and the spacetime metric for sound is then a *derived* and not fundamental (also see below). In the above relation (4),  $\Phi$  is a velocity potential due to the irrotationality of the superfluid (excluding quantized vortex lines). The scalar potential  $V_{\text{ext}}$  is employed by the cold quantum gas experimentalist to create certain classes of effective spacetimes (see for an overview [21]), while the condensate pressure  $p$  arises from the two-body repulsive contact interaction between atoms, where the coefficient  $g$  is proportional to the  $s$ -wave scattering length in the dilute gas [66]. Finally, the term  $\frac{\hbar^2}{2} \nabla \left( \frac{\nabla^2 \sqrt{\rho}}{\sqrt{\rho}} \right)$  in the Euler equation (2), is the so-called quantum pressure term [66]. From the barotropic equation of state (3), the sound speed  $c_s = \sqrt{\frac{dp}{d\rho}} = \sqrt{g\rho}$ ; stability implies that  $g > 0$ . We linearize the fluid equations over the background of a dispersive shock wave in a BEC [67]. The quantum pressure term is negligible until the shock is closely approached. Due to the quantum pressure term, the discontinuity in the flow, which were expected to be present in the nondispersive postshock phase [65], is regularized. One observes instead an oscillation pattern in the density profile upon approaching the shock (Fig. 5 in Appendix B). To *physically* distinguish classical sound wave from the background, one works with a linear perturbation with different space and time scale than the background flow, as discussed in the literature for linear sound propagation over background [21], and for nonlinear sound as well [63]. We denote background quantities with subscript (0) and the linear perturbations with subscript (1). We write  $\mathbf{v} = \mathbf{v}_{(0)} + \nabla \Phi_{(1)}$  by following the conventions of Ref. [63]. For example, with a dispersive nonlinear wave as the background, initially, when  $t$  is much less than the shock time  $t_{\text{shock}}$ , the wave is linear and nondispersive. For  $t \ll t_{\text{shock}}$ , such a linear wave satisfies the massless Klein-Gordon (KG) field equation over the analog Minkowski spacetime of a uniform static medium as background. We call this the *initial* background, and denote it with subscript 0. According to the Riemann wave equation for travelling one-dimensional (1D) waves, see Eq. (12) below, the intrinsic nonlinearity of the fluid-dynamical equations becomes significant in the course of time as the wave approaches the shock [65]. The KG analogy then does not hold anymore. In Ref. [63], we have described the classical backreaction of the nonlinear perturbation onto the acoustic metric, and defined a *new* background by absorbing these nonlinear perturbations into it. Here, we go near and beyond the shock time, with now in addition the quantum pressure, which originates from the spatial stiffness of the macroscopic BEC wave function against deformations, becoming significant. Linearizing (1) gives

$$\frac{\partial \rho_{(1)}}{\partial t} + \nabla \cdot (\rho_{(0)} \nabla \Phi_{(1)} + \rho_{(1)} \mathbf{v}_{(0)}) = 0. \quad (5)$$

The linearized Euler equation follows from the Eq. (2):

$$\begin{aligned} \dot{\Phi}_{(1)} + \frac{c_{s(0)}^2}{\rho_{(0)}} \rho_{(1)} + \mathbf{v}_{(0)} \cdot \nabla \Phi_{(1)} \\ + \frac{\hbar^2 \rho_{(1)}}{4\rho_{(0)}^2} \left( \nabla^2 \rho_{(0)} - \frac{1}{\rho_{(0)}} (\nabla \rho_{(0)})^2 \right) \\ + \frac{\hbar^2}{4\rho_{(0)}} \left( \frac{1}{\rho_{(0)}} \nabla \rho_{(0)} \cdot \nabla \rho_{(1)} - \nabla^2 \rho_{(1)} \right) = 0. \end{aligned} \quad (6)$$

Incorporating only the gradient terms from the background, thus neglecting  $\nabla \rho_{(1)}$ , and  $\nabla^2 \rho_{(1)}$ , we get

$$\rho_{(1)} \frac{(1 + \hbar^2 \alpha) c_{s(0)}^2}{\rho_{(0)}} = -\dot{\Phi}_{(1)} - \mathbf{v}_{(0)} \cdot \nabla \Phi_{(1)}. \quad (7)$$

Here, we introduced a parameter  $\alpha$  via

$$\alpha = \frac{1}{4c_{s(0)}^2} \nabla \cdot \left( \frac{\nabla \rho_{(0)}}{\rho_{(0)}} \right). \quad (8)$$

We can then define a new length scale  $l = l(x, t)$  via  $l^{-2} := \hbar^2 |\alpha| / \xi^2$  which characterizes the background spatial variation, and where the spatiotemporally local healing length is given by  $\xi(x, t) = \xi(\rho_{(0)}) = \frac{\hbar}{\sqrt{g\rho_{(0)}}}$

The competition of the ‘‘microscopic’’ structure dictated by  $\xi$  and the ‘‘background’’ scale  $l$  is expressed by  $\alpha(x, t)$  which thus appears in the metric  $q_{\mu\nu}$  in Eq. (9) below.

### B. Spacetime metric in the dispersive fluid

Now, we substitute  $\rho_{(1)}$  from Eq. (7) into Eq. (5), dropping the terms in the last closed bracket of Eq. (6). This is the limit where the linear perturbation of all physical quantities such as  $\rho_{(1)}$ ,  $p_{(1)}$  can be written in terms of partial derivatives in  $\Phi_{(1)}$ , and the full solution can be obtained when  $\Phi_{(1)}$  over a known background has been solved for. Going beyond this limit requires to solve for  $\rho_{(1)}$  also, and the equation of motion for  $\Phi_{(1)}$  becomes an integro-differential equation [41]. As a result, the acoustic spacetime metric is not local in space and time anymore. Here, we restrict ourselves to small wave number  $k$  excitations, i.e., perturbations with wavelength larger than the coherence length  $\xi(\rho_{(0)})$ . In this limit, we can construct an acoustic metric local in spacetime.

Linearizing in the perturbation amplitude now proceeds still as conventionally carried out in the analog gravity literature [20,21]. The difference is found in the dispersive nature of the background. The latter is controlled by well-posed initial (and/or boundary) conditions by the experimentalist. Over such an externally fixed, albeit nonlinear and dispersive background, any excitation to linear order is called a perturbation. In our particular case, the highly

TABLE I. Defining background flows from nonlinearity and dispersion and their associated metrics, where  $l$  is the length scale defined below (8). For Background (i),  $\rho_0, \mathbf{v}_0$  represent a solution of the nondispersive fluid equations without quantum pressure, and are initially chosen as the background before the shock develops, with perturbations treated to linear order. This initial Background (i) corresponds to the conventional analog gravity metric and may or may not derive from nonlinear fluid equations; for example, a uniform static medium does not represent a nonlinear background. For the **Background (ii)**,  $\rho_{(0)}, \mathbf{v}_{(0)}$ , are found from the fully nonlinear, coupled fluid equations for both background and perturbations, however without quantum pressure included. Cf. Ref. [63]. Finally, for the Background (iii),  $\rho_{(0)}, \mathbf{v}_{(0)}$  are found from the nonlinear fluid equations applied to the background motion alone, but now with quantum pressure included.

| Background (i)         | <b>Background (ii)</b>         | Background (iii)               |
|------------------------|--------------------------------|--------------------------------|
| $\rho_0, \mathbf{v}_0$ | $\rho_{(0)}, \mathbf{v}_{(0)}$ | $\rho_{(0)}, \mathbf{v}_{(0)}$ |
| $l \gg \xi$            | $l \gg \xi$                    | $l \sim \xi$                   |
| $g_{\mu\nu}$           | $\mathfrak{g}_{\mu\nu}$        | $q_{\mu\nu}$                   |

nonlinear and dispersive background flow is clearly distinct from the linear nondispersive perturbations which experience the effective spacetime produced from such a background medium. We then compare the equation of the scalar field  $\Phi_{(1)}$  to that of a minimally coupled massless KG field equation, and find the following effective spacetime metric in 3 + 1D,

$$q_{\mu\nu} := \frac{\rho_{(0)}}{c_{(0)}} \begin{bmatrix} -(c_{(0)}^2 - v_{(0)}^2) & \vdots & -\mathbf{v}_{(0)}^T \\ \cdots & \cdots & \cdots \\ -\mathbf{v}_{(0)} & \vdots & \mathbb{I}_{3 \times 3} \end{bmatrix}, \quad (9)$$

with a modified local sound speed

$$c_{(0)} = c_{s(0)} \sqrt{1 + \hbar^2 \alpha}, \quad (10)$$

due to the dispersive nature of the background. Evidently, the  $\hbar^2$  small length scale correction term is present for a general background flow. Note that for stability, we have to impose the lower bound  $\alpha > -1/\hbar^2$ .

The  $q_{\mu\nu}$  are no longer simple algebraic functions of background density and velocity, and interpolate between the fully nonlinear metric without dispersion  $\mathfrak{g}_{\mu\nu}$  introduced in [63] and the linear perturbations metric without dispersion  $g_{\mu\nu}$ . See Table I for an overview of the various concepts and the classification of spacetime metrics in the presence of nonlinearity and/or dispersion due to quantum pressure. We note that the effective spacetime metric for linear perturbations of wavelength larger than the healing length,  $q_{\mu\nu}$ , does not represent a so-called rainbow spacetime [68,69]. Distinct from such a rainbow spacetime, the metric  $q_{\mu\nu}$  does not depend on the wave vector  $k$  of the excitations.

### III. DISPERSIVE SHOCK WAVES

We consider the propagation of a wave, initially created as a Gaussian distribution, in the condensate. We consider a realistic situation, with the effect of quantum pressure included, i.e., a highly nonlinear dispersive wave [67]. The acoustic metric of such nonlinear dispersive pulse wave in our quasi-1D BEC set up, is given by the Eq. (9) with  $\mathbf{v}_{(0)}$  having only one component along the  $x$  axis,  $v_{(0)}(x, t)$ .

We choose the initial wave profile [67] as the Gaussian

$$\begin{aligned} \rho_{(0)}(x, t = 0) &= \rho_{\infty} \left( 1 + 2\eta \exp \left[ -\frac{x^2}{2\sigma^2} \right] \right), \\ v_{(0)}(x, t = 0) &= 0, \end{aligned} \quad (11)$$

where  $\sigma \gg \xi(\rho_{(0)})$ . Here, at the center of our quasi-1D BEC set up, we produce a source of gravitational wave (GW) with density being almost uniform towards the boundary, mimicking asymptotically flat effective spacetime with a GW source. This longitudinal GW is different from its counterpart in Einstein gravity, in that the spacetime lacks general covariance, and the GW cannot be represented in its usual transverse and traceless form, cf. the discussion in [61].

The Thomas-Fermi profile in Eq. (11) (neglecting the impact of quantum pressure on the initial state) can be created by focusing a laser detuned from atomic resonance onto the center of the one-dimensional condensate, with a size  $\gg \sigma$  [67]. Switching off the laser creates a nonlinear dispersive propagating wave with high frequency oscillations when the shock occurs, as previously described in [67], see for a detailed description Appendix B. Shock waves in quasi-1D BECs have been experimentally observed [70], and also in nonlinear photon fluids [71]. In particular, Ref. [70] captures density modulations which may be compared to the high-frequency postshock oscillations predicted by Damski [67].

We numerically solve the fluid equations (in a box potential with  $\nabla V_{\text{ext}} = 0$ ), that is Eqs. (1)–(4), employing a 4th order Runge-Kutta method to perform the time integration, and expanding the spatial derivatives within a central difference method scheme up to the same 4th order accuracy [72]. We now consider only nonlinearity taken into account for the fluid motion, i.e., Eqs. (1)–(4) without quantum pressure, and with the initial profile of Eq. (11). After a certain time, the initial Gaussian density wave profile separates completely into two identical smaller pieces (while respecting mass conservation), and moving in opposite directions. The right-moving traveling wave in the polytropic gas with pressure  $p_{(0)} \propto \rho_{(0)}^{\gamma}$  (for BECs  $\gamma = 2$ ) can be described in terms of single variable  $v_{(0)}(x, t)$  by the Riemann wave equation [73]:

$$\frac{\partial v_{(0)}}{\partial t} + \left[ c_{s0} + \left( \frac{\gamma + 1}{2} \right) v_{(0)} \right] \frac{\partial v_{(0)}}{\partial x} = 0, \quad (12)$$

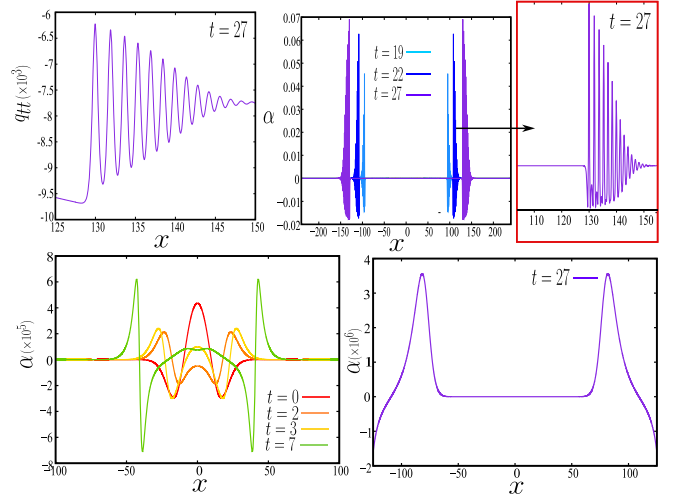


FIG. 1. Behavior of  $q_{\mu\nu}$  for the dispersive shock wave as background, found by numerically solving Eqs. (1)–(4). We use here units in terms of a length  $L$ , chosen appropriately for the purpose of our numerical calculation. For example, in the experiment [70] the size of the condensate is roughly  $500 \mu\text{m}$ , whereas the full  $x$ -axis range of our numerical simulation is 500. Therefore  $L$  would be approximately  $1 \mu\text{m}$  with the parameters of Ref. [70]. Time  $t$  is then measured in units of  $L^2$ , when setting  $\hbar = 1$ . In these units, the parameters we choose are  $g = 7500$ ,  $\rho_{\infty} = 0.002$ ,  $\eta = 0.2$ ,  $\sigma = 8.838$ . We then obtain  $t_{\text{shock}} \simeq 13.43$ , using the method described in Ref. [67]. Only after and slightly before the instant of shock, the dispersive nature of the background flow becomes important in the oscillatory region, and hence in  $q_{\mu\nu}$ . Top left (at  $t = 27$ ): We plot  $q_H$  in the postshock phase; the behavior of other metric components is similar. (Bottom row): In the postshock phase, the amplitude of the parameter  $\alpha$  defined in Eq. (8) in the nonoscillatory region is essentially negligible compared to its amplitude in the oscillatory region; it, however, increases rapidly as  $t$  approaches  $t_{\text{shock}}$ .

$$\rho_{(0)} = \rho_0 \left[ 1 + \left( \frac{\gamma - 1}{2} \right) \frac{v_{(0)}}{c_{s0}} \right]^{\frac{2}{\gamma-1}}. \quad (13)$$

The second identity directly relating density to flow speed perturbations is valid for a *simple wave* [65]. The left-moving traveling wave comes with a  $-$  sign in front of  $c_{s0}$  in the above equations;  $\rho_{(0)} = \rho_{\infty}$  for  $v_{(0)} = 0$ ,  $\rho_{\infty} \simeq \rho_0$  of Eq. (11) since  $\sigma \ll$  size of the condensate. This first-order quasilinear partial differential equation leads to multivalued valued solution by the method of characteristics [74].

By obeying momentum and mass conservation across the discontinuity, one is led to the equal area rule  $\oint (x - x_s) dv_{(0)} = 0$  where  $x_s$  is the shock location (location of discontinuity), to avoid such a multivalued solution from the shock time ( $=t_{\text{shock}}$ ) onward [65]. We discuss this issue further in Appendix A. In the presence of quantum pressure, the solution (density, velocity, etc.) becomes oscillatory around the discontinuity, in comparison in Fig. 2. Therefore, the solution becomes a *well behaved* function of  $x$  and  $t$  [67], see Appendix B. The numerical

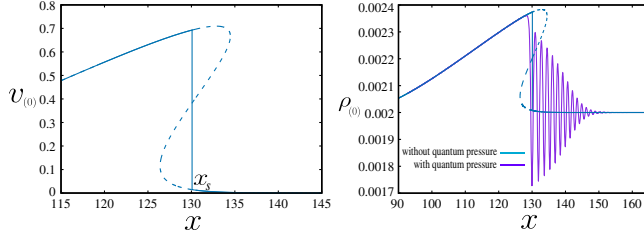


FIG. 2. (Left) Multivalued solution of postshock Riemann wave by the method of characteristics (dotted): physical solution with discontinuity (nondispersive shock) and by equal area rule [65] (solid line). (Right) Discontinuity in the flow is avoided as the wave approaches the shock time when we take quantum pressure into account. Inclusion of quantum pressure in the equation creates oscillation and thus continuous solution of  $v_{(0)}$  removes singularity in the acoustic metric, i.e., censorship of singularity. The wave profile with quantum pressure is a good match with the nondispersive nonlinear wave profile in the region except the rapidly oscillatory region. Parameters as in Fig. 1.

solution of Eq. (1) together with Eq. (4) produces  $q_{tt}$  in Fig. 1. As expected,  $\alpha$  is practically zero in the non-oscillatory region. The  $\alpha$ -correction term in the metric  $g_{\mu\nu}$ , which is usually hidden in a slowly varying background, is amplified in a region where quantum pressure is important: It is a significant contribution relative to the other forces in the Euler-type evolution of momentum (2) in the oscillatory region (cf. Fig. 7 in the Appendix B). Remarkably, the oscillations in the solution starts just slightly before the shock time  $t_{\text{shock}}$  (see Fig. 6 in Appendix B), whereas  $t_{\text{shock}}$  is computed in the zero quantum pressure limit. Therefore,  $t_{\text{shock}}$  maintains its importance as a timescale even with quantum pressure, signifying the time of initiation of oscillation. A linear traveling 1D wave cannot stay linear forever; after a certain time nonlinearity makes the  $v_{(0)}$  profile steeper, with negative  $\frac{\partial v_{(0)}}{\partial x}$ . This renders, in turn, the quantum pressure significant. Thus nonlinearity invites dispersion due to quantum pressure to play a significant role, also see the Appendices A and B.

#### IV. CENSORING THE NAKED SINGULARITY

We now aim to find what a discontinuity in the solution means for the effective spacetime. We denote the acoustic metric for the nondispersive metric as  $\mathfrak{g}_{\mu\nu}$ , cf. Table I. We stress that, while the metric is derived nondispersively, it is still taking the nonlinearity of the fluid into account [63]. It reads

$$ds^2 = \mathfrak{g}_{\mu\nu} dx^\mu dx^\nu = \frac{\rho_{(0)}}{c_{s(0)}} \left[ -(c_{s(0)}^2 - v_{(0)}^2) dt^2 - 2v_{(0)} dt dx + \sum_{i=1,2,3} (dx^i)^2 \right]. \quad (14)$$

Note that this metric is also *not* identical to the conventional analog gravity metric  $g_{\mu\nu}$ , which assumes that the dynamics

of perturbations is linear instead of nonlinear, cf. Table I for a classification of metrics. The linear approximation is valid only for small amplitudes and short time intervals, while the quantities  $\rho_{(0)}$ ,  $v_{(0)}$  in the metric are found from the solution of the nonlinear fluid equations without quantum pressure. This is **Background (i)** in Table I. For nonlinear dispersive shock wave, **Background (ii)** and Background (iii) coincide very well in every region except in the oscillatory region, i.e., the region around shock location  $x_s$ . In the asymptotic region, i.e., near the condensate wall, **Background (ii)** and Background (iii) coincide with the Background (i) which is uniform and static, i.e., an acoustic analog of Minkowski spacetime.

Evidently the acoustic metric is discontinuous at  $x = x_s$  after the shock has occurred. We compute the Ricci scalar,  $R$  [75] for  $\mathfrak{g}_{\mu\nu}$  for the right-moving traveling wave satisfying Eq. (12). We perform the calculations in *Mathematica*, replacing  $\partial_t$  by  $\partial_x$  derivatives, employing the Riemann wave equation (12). This procedure leads to the surprisingly simple relation

$$R = \frac{(1 + \gamma)}{\rho_{(0)}} \frac{\partial^2 v_{(0)}(x, t)}{\partial x^2}, \quad (15)$$

expressing the curvature scalar solely by the second spatial derivative of the background flow field. At  $x = x_s$ ,  $v_{(0)} = v_1$ , and  $\rho_{(0)} = \rho_1$ , which are the preshock values of velocity and density, respectively, related to each other by Eq. (13). Since, in this case the wave is propagating from left to right, at  $x = x_s$ ,  $v_{(0)}$  first has  $v_1$  then it jumps to postshock value  $v_2 (< v_1)$ , thus unrealistic multivalued  $v_{(0)}$  is avoided.  $\lim_{x \rightarrow x_s} v_{(0)}(x, t)$  does not exist, but it has a definite value which is  $v_1$ , and as a consequence; this discontinuity can be written mathematically in terms of a Heaviside step function, see Appendix A.  $\frac{\partial v_{(0)}(x, t)}{\partial x} = -\infty$  at  $x = x_s$ , and  $\frac{\partial^2 v_{(0)}(x, t)}{\partial x^2}$  at  $x = x_s$  can be expressed as a summation of  $\delta(0)$  and  $\delta'(0)$  (with definite coefficients) type of infinities (in Appendix A); where  $'$  denotes a  $x$  derivative. We discuss the visualization of Dirac delta distributions through a delta-sequence function in Fig. 4 of Appendix A.

We plot in Fig. 3 the Ricci scalar of the nondispersive wave as it approaches the curvature singularity in the preshock phase  $t < t_{\text{shock}}$ . As can be seen, the expression (15) implies the existence of a (strong) curvature singularity at  $x = x_s$ , where  $x_s$  is the position of discontinuity at  $t \geq t_{\text{shock}}$ . Since the velocity at any  $x$  remains always very much less than the minimum value of sound speed  $c_{s0}$  ( $= \sqrt{g\rho_0}$ ), there is no event horizon present in the acoustic metric. Since at  $x = x_s$ ,  $v_{(0)} = v_1$ ; sound speed  $c_{s(0)} = c_{s1} = c_{s0} + \left(\frac{\gamma+1}{2}\right)v_1$ , and the travel speed of the discontinuity is  $u = c_{s0} + \left(\frac{\gamma+1}{4}\right)(v_1 + v_2)$ ,  $v_2 (< v_1)$  is

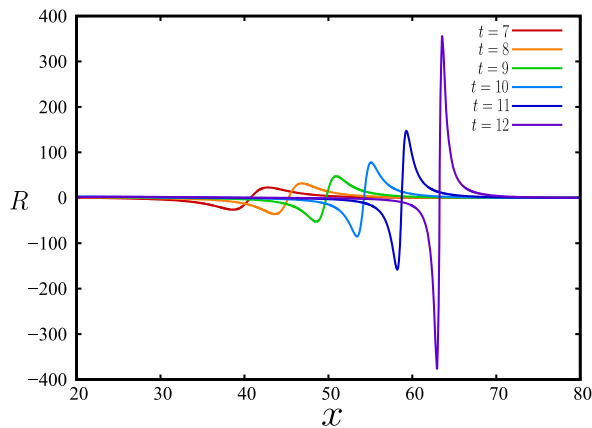


FIG. 3. Time evolution of the Ricci scalar of  $g_{\mu\nu}$  in Eq. (15), when approaching the shock singularity of the nondispersive Riemann wave. Parameters are identical to those of Fig. 1.

the postshock value of  $v_{(0)}$  [65]. Hence  $c_{s1} > u$ . In Eq. (14), by putting  $dx = udt$ ,  $dy = dz = 0$ , we find  $ds^2 = \frac{dt^2}{c_{s1}^2} (-c_{s1}^2 + (u - v_1)^2) dt^2$ , from the above discussion, we notice that  $c_{s1} > |u - v_1|$ . Therefore, at  $x = x_s$ , the discontinuity follows a timelike trajectory, representing a naked singularity. When we, on the other hand, solve the fluid equations with quantum pressure, the solution oscillates instead of discontinuity; we render the curvature for the metric  $q_{\mu\nu} \forall x$  and  $t$  finite, thus removing the singularity, cf. Fig. 2. However, for nondispersive waves, the discontinuity does not persist for  $t \rightarrow \infty$ , and  $(v_1 - v_2)$  then falls to zero [65].

## V. COMPARISON WITH HYDRAULIC JUMP

To put the above discussion on dispersively censoring shock-wave spacetime singularities in perspective, we compare it with another example for a possible spacetime singularity, the so-called hydraulic jump [76].

In general relativity, the components of the spacetime metric reflect a choice of coordinate system, and there is no preferred coordinate system. Hence constructing scalar quantities, such as the Ricci scalar, quantifying the curvature is important to distinguish genuine spacetime singularities from singularities removable by coordinate transformations. However, the acoustic metric components for analog gravity (in the present nonrelativistic background framework) are functions of physical quantities (velocity and density of the background flow). Then, a discontinuity in the acoustic metric can also be regarded as a *physical* singularity, i.e., some kind of boundary between two different spacetime manifolds. Therefore, the singularity for the postshock simple wave is not only a Ricci scalar curvature singularity at  $x = x_s$ , but also can be regarded as the boundary between two different manifolds with two distinct acoustic spacetime metric defined on them.

The hydraulic jump possesses a *physical* singularity at an effective radial white hole horizon (for the circular hydraulic jump), as represented by a sudden increase in fluid height at the circular boundary [77]. The white-hole horizon for the circular jump has, for example, been experimentally studied for viscous silicon oil with low surface tension (and with therefore no capillary dispersion) [78]. Distinct from the singularity for shock wave, the singularity for the hydraulic jump is neither naked nor hidden behind a horizon, as the hydraulic jump spacetime singularity occurs exactly at the horizon [77]. If the hydraulic jump is “noticeably” sharp, as observed in liquid helium [79] as well as in viscous silicon oil [78], such a jump can indeed be considered a *physical* singularity. However, the continuum approximation in fluid dynamics is valid after coarse graining over a certain length scale. For example, in the case of the flow of a real gas, the fluid descriptions of physical quantities such as velocity and density are valid on a length scale much bigger than the mean free path of the constituent particles. Similarly, for a BEC with quantum pressure included, the number of atoms per healing length has to be much greater than unity for the mean-field hydrodynamical description to apply. Therefore, the description in terms of a spacetime singularity due to a discontinuity in the background flow holds on the length scales for which fluid dynamics is valid.

In rectangular channel flows, the jump in fluid height is however noticeably smooth instead of sharp [80,81], and for narrow channel flow, the hydraulic jump is followed by a post-jump undulation, constituting the so-called *undular* hydraulic jump [82,83]. The undular hydraulic jump has been studied in viscous flows, e.g., in [84], as well as turbulent flows, e.g., in [85]. The dissipation due to turbulence and viscosity for the channel undular hydraulic jump prevents a sharp rise in fluid height.

The dispersive shock wave problem that we consider here for a BEC is structurally similar to the Korteweg–De Vries equation, which includes nonlinearity and dispersion [86,87]. In our case, the dispersion is due to quantum pressure, which modifies the acoustic metric Eq. (9), and, as a consequence, resolves the singularity in the metric. By contrast, the undular jump in channel flows involves dissipation in addition, which is complicating its analysis.

To summarize, in distinction to the (undular) hydraulic jump, in our simplified 1D shock-wave setup we have no turbulence (flow speeds remaining well below the speed of sound), and no spacetime horizon. We also have no dissipation for a BEC at  $T = 0$ . Finally, the dispersion we consider in a BEC, while in the shallow water limit formally similar to quartic order in wave number, has a different physical origin than for the hydraulic jump [78]. Finally, as far as we are aware, our study presents the first confirmation of a *spacetime* singularity by explicitly

calculating the corresponding divergence of the Ricci curvature scalar.

## VI. CONCLUSION

We demonstrated that the quantum pressure term leads to a regular oscillatory numerical solution for traveling waves in a quasi-1D BEC, thus prohibiting the otherwise naked singularity. Analog gravity is effectively an aether theory, for which we have shown, using a particular initial condition, that the occurrence of a naked singularity is forbidden. Whether singularities in the dispersive aether of the BEC arise for *any* given nonsingular initial condition is an open question.

We have thus provided, for a BEC laboratory analog simulating curved spacetimes, a censor prototype operating in the trans-Planckian sector of the dispersion relation, which is based on the microscopic physics of the system, and is thus naturally complete in the ultraviolet. To ultimately resolve the question of whether the CCH holds true, this latter property is crucial also for any proper quantum gravity.

## ACKNOWLEDGMENTS

We thank B. Damski and F. Marino for helpful discussions on dispersive shock waves. This work has been supported by the National Research Foundation of Korea under Grants No. 2017R1A2A2A05001422 and No. 2020R1A2C2008103.

## APPENDIX A: NONDISPERSIVE SHOCK WAVES AND THE CURVATURE SINGULARITY

In this appendix, first we briefly introduce the equal area principle introduced in [65] for nondispersive shock waves, and then we proceed to calculating the Ricci scalar curvature for such a nondispersive shock wave.

The Riemann wave equation (12) can be solved by the analytical techniques for partial differential equations, i.e., the method of characteristics. This analytical solution [61] gives rise to multivalued solution after a certain time,  $t_{\text{shock}}$ . At  $t = t_{\text{shock}}$ ,  $\frac{\partial v_{(0)}}{\partial x}$  reaches infinity [65]. If we follow the method of characteristics [63,65] to solve Eq. (12) for the case without quantum pressure to avoid multivalued solution of density and velocity after  $t_{\text{shock}}$ , the solution has to become discontinuous. This jump in velocity (and density) approximately satisfies the equal area rule [65]:

$$\int_{v_1}^{v_2} (x - x_s) dv_{(0)} = 0, \quad (\text{A1})$$

where  $v_1$  and  $v_2$  ( $v_1 > v_2$ ) are the preshock and postshock values of discontinuous velocity  $v_{(0)}$  across the position of discontinuity (shock) at  $x = x_s$ . As a result,  $\rho_1$  and  $\rho_2$  are preshock and postshock values of density  $\rho_{(0)}$  related to  $v_1$  and  $v_2$  by

$$\rho_{1,2} = \rho_0 \left[ 1 + \left( \frac{\gamma - 1}{2} \right) \frac{v_{1,2}}{c_{s0}} \right]^{\frac{2}{\gamma-1}}. \quad (\text{A2})$$

With this discontinuity, velocity and density profiles are not multivalued anymore, which is discussed in detail by the classic textbook [65]. The expression of Ricci scalar [Eq. (15)] in the nondispersive limit is proportional to the second derivative in  $v_{(0)}$ , here we discuss an analytical way to calculate the second derivative of  $v_{(0)}$  with a discontinuity at  $x = x_s$ . This discontinuous velocity profile  $v_{(0)}(x, t)$  at fixed time  $t > t_{\text{shock}}$  can be written in a compact approximate way,

$$v_{(0)}(x, t) = (1 - \Theta(x - x_s))f_1(x) + \Theta(x - x_s)f_2(x), \quad (\text{A3})$$

where  $\Theta$  is the Heaviside step function, defined by  $\Theta(x - x_s) = 1$  for  $x > x_s$  and  $\Theta(x - x_s) = 0$  for  $x \leq x_s$ . Furthermore,  $f_1(x)$ ,  $f_2(x)$  are Newton interpolation polynomials [72], constructed from a finite number of points on the preshock curve segment and on the postshock curve segment of  $v_{(0)}(x, t)$ , respectively, at a fixed time  $t > t_{\text{shock}}$ , e.g., from the left of Fig. 2. Thus we approximately describe  $v_{(0)}(x, t)$  at fixed  $t > t_{\text{shock}}$  by these two polynomials with finite coefficients in a compact way. Therefore,  $f_1(x)$  and  $f_2(x)$ , for a *reasonably accurate* fitting, should satisfy (a)  $f_1(x_s) \sim v_1 > f_2(x_s) \sim v_2$ , and (b) the slopes of  $f_1(x)$  and  $f_2(x)$ , at  $x = x_s$  *smoothly* fits into the preshock curve segment and postshock curve segment, respectively. We find

$$\begin{aligned} \frac{\partial v_{(0)}}{\partial x} &= (1 - \Theta(x - x_s)) \frac{df_1}{dx} + \Theta(x - x_s) \frac{df_2}{dx} \\ &+ \delta(x - x_s)(f_2(x) - f_1(x)), \end{aligned} \quad (\text{A4})$$

where  $\delta(x - x_s)$  is the Dirac delta distribution. The first two finite terms of the equation has a similar pattern to the Eq. (A3) for obvious reasons. Therefore,

$$\left. \frac{\partial v_{(0)}}{\partial x} \right|_{x=x_s} = \delta(0)(v_2 - v_1) + \left. \frac{df_1}{dx} \right|_{x=x_s}. \quad (\text{A5})$$

Evidently, the first term on the right-hand side dominates over the second term, rendering  $\left. \frac{\partial v_{(0)}}{\partial x} \right|_{x=x_s}$  to be  $-\infty$ , since  $v_2 < v_1$ .

$$\begin{aligned} \frac{\partial^2 v_{(0)}}{\partial x^2} &= (1 - \Theta(x - x_s)) \frac{d^2 f_1}{dx^2} + \Theta(x - x_s) \frac{d^2 f_2}{dx^2} \\ &+ 2\delta(x - x_s) \left( \frac{df_2}{dx} - \frac{df_1}{dx} \right) \\ &+ \delta'(x - x_s)(f_2(x) - f_1(x)). \end{aligned} \quad (\text{A6})$$

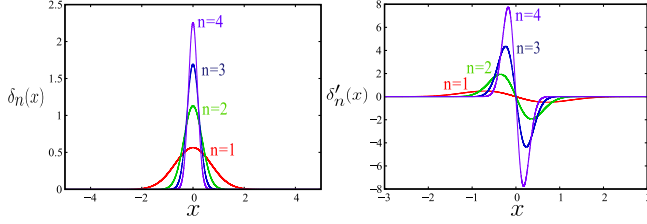


FIG. 4. Sequences up to  $n = 4$  are shown to represent the delta distribution function (left) and its first derivative (right).  $\lim_{n \rightarrow \infty} \int_{-\infty}^{\infty} f(x) \delta_n(x) dx = \int_{-\infty}^{\infty} f(x) \delta(x) dx$ , and  $\lim_{n \rightarrow \infty} \int_{-\infty}^{\infty} f(x) \delta'_n(x) dx = \int_{-\infty}^{\infty} f(x) \delta'(x) dx$  [for arbitrary  $f(x)$ ] are used to define a relation of the Dirac delta distribution and its derivative with their respective sequence functions [88].

Therefore, at  $x = x_s$ , ignoring the finite term  $\frac{d^2 f_1}{dx^2} \Big|_{x=x_s}$ , we write down the infinite terms as follows:

$$\frac{\partial^2 v(0)}{\partial x^2} \Big|_{x=x_s} = 2\delta(0) \left( \frac{df_2}{dx} \Big|_{x=x_s} - \frac{df_1}{dx} \Big|_{x=x_s} \right) + \delta'(0)(v_2 - v_1). \quad (\text{A7})$$

According to Fig. 2,  $\frac{df_2}{dx} \Big|_{x=x_s}$  is negative; it always stays negative in the postshock phase, and  $\frac{df_1}{dx} \Big|_{x=x_s}$  is positive. Numerics in fact shows that, initially after  $t_{\text{shock}}$ ,  $\frac{df_1}{dx} \Big|_{x=x_s}$  is negative, but eventually it becomes positive over time. The quantity  $\frac{\partial^2 v(0)}{\partial x^2} \Big|_{x=x_s}$  above consists of two different kinds of infinity. One can represent them by  $\delta$ -sequence functions [88]. We choose here a particular one to describe these infinities (see also Fig. 4),

$$\delta_n(x) = \frac{n}{\sqrt{\pi}} \exp(-n^2 x^2), \quad (\text{A8})$$

$$\delta'_n(x) = -\frac{2n^3 x}{\sqrt{\pi}} \exp(-n^2 x^2), \quad (\text{A9})$$

where  $n$  is a positive integer. Using the relations  $x\delta'(x) = -\delta(x)$  and  $x^2\delta'(x) = -x\delta(x) = 0$ , we observe from Eq. (A6)

$$\begin{aligned} (x - x_s) \frac{\partial^2 v(0)}{\partial x^2} &= (x - x_s)(1 - \Theta(x - x_s)) \frac{d^2 f_1}{dx^2} \\ &+ (x - x_s)\Theta(x - x_s) \frac{d^2 f_2}{dx^2} \\ &- \delta(x - x_s)(f_2(x) - f_1(x)). \end{aligned} \quad (\text{A10})$$

Then it follows that

$$(x - x_s)^n \frac{\partial^2 v(0)}{\partial x^2} \Big|_{x=x_s} = -\delta_{n,1} \delta(0)(v_2 - v_1). \quad (\text{A11})$$

This is how “strange” the second derivative  $\frac{\partial^2 v(0)}{\partial x^2} \Big|_{x=x_s}$  in fact behaves.

## APPENDIX B: INITIATION OF OSCILLATIONS IN DISPERSIVE SHOCK WAVES

In this appendix, we collect our numerical findings on dispersive shock waves with initial conditions (11), as described in the main text. Some of these results have been presented already in Ref. [67], but for the convenience of the reader we reproduce here these results together with a few additional observations, where our overall aim is to inspect closely the initiation of the oscillation of the

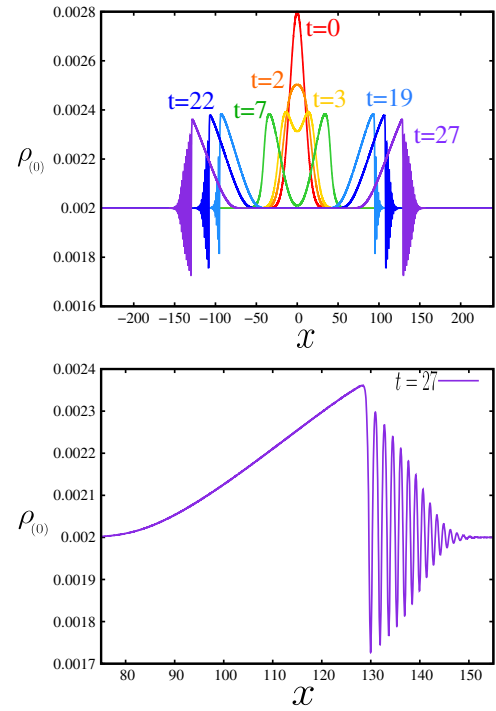


FIG. 5. (Top) Evolution of density profile with time. At  $t = 0$ , the laser at the center of the condensate is switched off. The initial Gaussian density profile splits in two parts, moving in opposite directions, and an oscillation pattern is created, as described in Ref. [67]. (Bottom) Zoomed-in view of the density profile in the oscillation region at  $t = 27$ . Parameters as in Fig. 1.

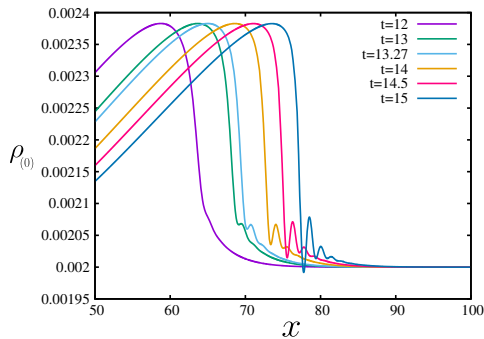


FIG. 6. Density near the shock time,  $t_{\text{shock}} \simeq 13.43$ . An oscillation starts instead of a discontinuity popping up, due to the presence of quantum pressure. The initial wave parameters are as in Fig. 1.

dispersive shock waves, which is due to the quantum pressure term.

Specifically, in Fig. 5, we observe how the oscillation region is slowly spreading with progressing time. In Fig. 6, we display how the shock wave enters the oscillation phase, just prior to the shock time  $t_{\text{shock}}$ . Finally, in Fig. 7, we display in some detail the onset of oscillations due to the quantum pressure becoming significant.

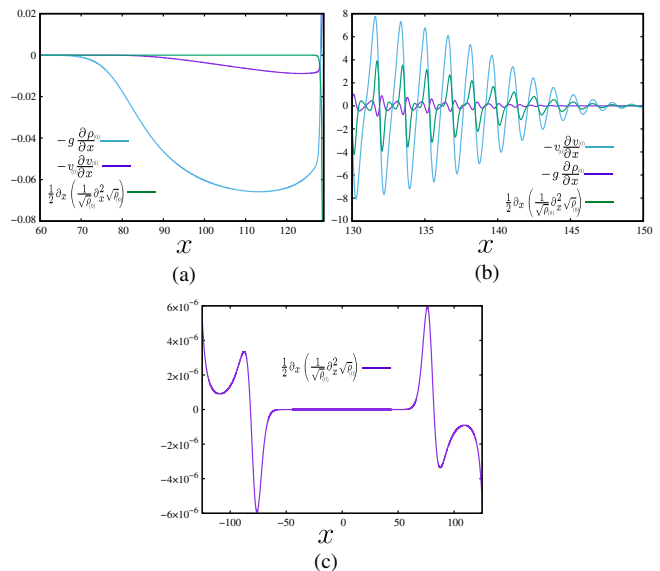


FIG. 7. (a) and (b) We compare the contribution of the terms involving derivatives in  $x$  in the 1D momentum equation (2) at  $t = 27$ . We see that the quantum pressure term becomes significant only in the oscillatory region. (c) The quantum pressure is very much smaller, by several orders of magnitude, in the nonoscillatory region. The parameters are identical to those in Fig. 1.

- [1] R. Penrose, Gravitational Collapse and Space-Time Singularities, *Phys. Rev. Lett.* **14**, 57 (1965).
- [2] R. Penrose, Gravitational collapse: The role of general relativity, *Riv. Nuovo Cimento* **1**, 252 (1969).
- [3] S. W. Hawking, Breakdown of predictability in gravitational collapse, *Phys. Rev. D* **14**, 2460 (1976).
- [4] S. W. Hawking and H. Bondi, The occurrence of singularities in cosmology, *Proc. R. Soc. A* **294**, 511 (1966).
- [5] S. W. Hawking and H. Bondi, The occurrence of singularities in cosmology. II, *Proc. R. Soc. A* **295**, 490 (1966).
- [6] S. W. Hawking, The occurrence of singularities in cosmology. III. Causality and singularities, *Proc. R. Soc. A* **300**, 187 (1967).
- [7] S. W. Hawking and R. Penrose, The singularities of gravitational collapse and cosmology, *Proc. R. Soc. A* **314**, 529 (1970).
- [8] R. Penrose, The question of cosmic censorship, *J. Astrophys. Astron.* **20**, 233 (1999).
- [9] R. M. Wald, Gravitational collapse and cosmic censorship, in *Black Holes, Gravitational Radiation and the Universe*, edited by B. R. Iyer and B. Bhawal (Springer, New York, 1999), pp. 69–86.
- [10] D. Christodoulou, Violation of cosmic censorship in the gravitational collapse of a dust cloud, *Commun. Math. Phys.* **93**, 171 (1984).
- [11] M. D. Roberts, Scalar field counterexamples to the cosmic censorship hypothesis, *Gen. Relativ. Gravit.* **21**, 907 (1989).
- [12] V. E. Hubeny, Overcharging a black hole and cosmic censorship, *Phys. Rev. D* **59**, 064013 (1999).
- [13] G. E. A. Matsas and A. R. R. da Silva, Overspinning a Nearly Extreme Charged Black Hole via a Quantum Tunneling Process, *Phys. Rev. Lett.* **99**, 181301 (2007).
- [14] G. E. A. Matsas, M. Richartz, A. Saa, A. R. R. da Silva, and D. A. T. Vanzella, Can quantum mechanics fool the cosmic censor?, *Phys. Rev. D* **79**, 101502(R) (2009).
- [15] S. Hod, Weak Cosmic Censorship: As Strong as Ever, *Phys. Rev. Lett.* **100**, 121101 (2008).
- [16] M. Casals, A. Fabbri, C. Martínez, and J. Zanelli, Quantum dress for a naked singularity, *Phys. Lett. B* **760**, 244 (2016).
- [17] R. Wald, Gedanken experiments to destroy a black hole, *Ann. Phys. (N.Y.)* **82**, 548 (1974).
- [18] J. Sorce and R. M. Wald, Gedanken experiments to destroy a black hole. II. Kerr-Newman black holes cannot be overcharged or overspun, *Phys. Rev. D* **96**, 104014 (2017).
- [19] S. Hod, Return of the quantum cosmic censor, *Phys. Lett. B* **668**, 346 (2008).
- [20] W. G. Unruh, Experimental Black-Hole Evaporation?, *Phys. Rev. Lett.* **46**, 1351 (1981).
- [21] C. Barceló, S. Liberati, and M. Visser, Analogue gravity, *Living Rev. Relativity* **14**, 3 (2011).
- [22] C. Barceló, S. Liberati, and M. Visser, Analogue gravity from field theory normal modes?, *Classical Quantum Gravity* **18**, 3595 (2001).

- [23] R. Schützhold and W. G. Unruh, Gravity wave analogues of black holes, *Phys. Rev. D* **66**, 044019 (2002).
- [24] S. Weinfurter, E. W. Tedford, M. C. J. Penrice, W. G. Unruh, and G. A. Lawrence, Measurement of Stimulated Hawking Emission in an Analogue System, *Phys. Rev. Lett.* **106**, 021302 (2011).
- [25] L.-P. Euvé, F. Michel, R. Parentani, T. G. Philbin, and G. Rousseaux, Observation of Noise Correlated by the Hawking Effect in a Water Tank, *Phys. Rev. Lett.* **117**, 121301 (2016).
- [26] L.-P. Euvé, S. Robertson, N. James, A. Fabbri, and G. Rousseaux, Scattering of Co-Current Surface Waves on an Analogue Black Hole, *Phys. Rev. Lett.* **124**, 141101 (2020).
- [27] F. Marino, Acoustic black holes in a two-dimensional “photon fluid”, *Phys. Rev. A* **78**, 063804 (2008).
- [28] H. S. Nguyen, D. Gerace, I. Carusotto, D. Sanvitto, E. Galopin, A. Lemaître, I. Sagnes, J. Bloch, and A. Amo, Acoustic Black Hole in a Stationary Hydrodynamic Flow of Microcavity Polaritons, *Phys. Rev. Lett.* **114**, 036402 (2015).
- [29] M. Jacquet, M. Joly, F. Claude, L. Giacomelli, Q. Glorieux, A. Bramati, I. Carusotto, and E. Giacobino, Analogue quantum simulation of the Hawking effect in a polariton superfluid, *Eur. Phys. J. D* **76**, 152 (2022).
- [30] T. Torres, S. Patrick, M. Richartz, and S. Weinfurter, Quasinormal mode oscillations in an analogue black hole experiment, *Phys. Rev. Lett.* **125**, 011301 (2020).
- [31] S. Datta, Acoustic analog of gravitational wave, *Phys. Rev. D* **98**, 064049 (2018).
- [32] S. Liberati, G. Tricella, and A. Trombettoni, The information loss problem: An analogue gravity perspective, *Entropy* **21**, 940 (2019).
- [33] S. Corley and T. Jacobson, Black hole lasers, *Phys. Rev. D* **59**, 124011 (1999).
- [34] A. Kosior, M. Lewenstein, and A. Celi, Unruh effect for interacting particles with ultracold atoms, *SciPost Phys.* **5**, 61 (2018).
- [35] S. Basak and P. Majumdar, ‘Superresonance’ from a rotating acoustic black hole, *Classical Quantum Gravity* **20**, 3907 (2003).
- [36] T. Torres, S. Patrick, A. Coutant, M. Richartz, E. W. Tedford, and S. Weinfurter, Rotational superradiant scattering in a vortex flow, *Nat. Phys.* **13**, 833 (2017).
- [37] A. Prain, C. Maitland, D. Faccio, and F. Marino, Superradiant scattering in fluids of light, *Phys. Rev. D* **100**, 024037 (2019).
- [38] M. C. Braidotti, R. Prizia, C. Maitland, F. Marino, A. Prain, I. Starshynov, N. Westerberg, E. M. Wright, and D. Faccio, Measurement of Penrose Superradiance in a Photon Superfluid, *Phys. Rev. Lett.* **128**, 013901 (2022).
- [39] M. Richartz, A. Prain, S. Liberati, and S. Weinfurter, Rotating black holes in a draining bathtub: Superradiant scattering of gravity waves, *Phys. Rev. D* **91**, 124018 (2015).
- [40] L. J. Garay, J. R. Anglin, J. I. Cirac, and P. Zoller, Sonic Analog of Gravitational Black Holes in Bose-Einstein Condensates, *Phys. Rev. Lett.* **85**, 4643 (2000).
- [41] C. Barceló, S. Liberati, and M. Visser, Analogue gravity from Bose-Einstein condensates, *Classical Quantum Gravity* **18**, 1137 (2001).
- [42] I. Carusotto, S. Fagnocchi, A. Recati, R. Balbinot, and A. Fabbri, Numerical observation of Hawking radiation from acoustic black holes in atomic Bose–Einstein condensates, *New J. Phys.* **10**, 103001 (2008).
- [43] J. Macher and R. Parentani, Black-hole radiation in Bose-Einstein condensates, *Phys. Rev. A* **80**, 043601 (2009).
- [44] O. Lahav, A. Itah, A. Blumkin, C. Gordon, S. Rinott, A. Zayats, and J. Steinhauer, Realization of a Sonic Black Hole Analog in a Bose-Einstein Condensate, *Phys. Rev. Lett.* **105**, 240401 (2010).
- [45] J. Steinhauer, Observation of quantum Hawking radiation and its entanglement in an analogue black hole, *Nat. Phys.* **12**, 959 (2016).
- [46] J. R. Muñoz de Nova, K. Golubkov, V. I. Kolobov, and J. Steinhauer, Observation of thermal Hawking radiation and its temperature in an analogue black hole, *Nature (London)* **569**, 688 (2019).
- [47] S.-Y. Chä and U. R. Fischer, Probing the Scale Invariance of the Inflationary Power Spectrum in Expanding Quasi-Two-Dimensional Dipolar Condensates, *Phys. Rev. Lett.* **118**, 130404 (2017).
- [48] S. Eckel, A. Kumar, T. Jacobson, I. B. Spielman, and G. K. Campbell, A Rapidly Expanding Bose-Einstein Condensate: An Expanding Universe in the Lab, *Phys. Rev. X* **8**, 021021 (2018).
- [49] S. Eckel and T. Jacobson, Phonon redshift and Hubble friction in an expanding BEC, *SciPost Phys.* **10**, 64 (2021).
- [50] S. Banik, M. G. Galan, H. Sosa-Martinez, M. J. Anderson, S. Eckel, I. B. Spielman, and G. K. Campbell, Accurate Determination of Hubble Attenuation and Amplification in Expanding and Contracting Cold-Atom Universes, *Phys. Rev. Lett.* **128**, 090401 (2022).
- [51] U. R. Fischer and R. Schützhold, Quantum simulation of cosmic inflation in two-component Bose-Einstein condensates, *Phys. Rev. A* **70**, 063615 (2004).
- [52] C. Barceló, S. Liberati, and M. Visser, Probing semiclassical analog gravity in Bose-Einstein condensates with widely tunable interactions, *Phys. Rev. A* **68**, 053613 (2003).
- [53] P. O. Fedichev and U. R. Fischer, “Cosmological” quasi-particle production in harmonically trapped superfluid gases, *Phys. Rev. A* **69**, 033602 (2004).
- [54] S. Robertson, F. Michel, and R. Parentani, Assessing degrees of entanglement of phonon states in atomic Bose gases through the measurement of commuting observables, *Phys. Rev. D* **96**, 045012 (2017).
- [55] C. Gooding, S. Biermann, S. Erne, J. Louko, W. G. Unruh, J. Schmiedmayer, and S. Weinfurter, Interferometric Unruh Detectors for Bose-Einstein Condensates, *Phys. Rev. Lett.* **125**, 213603 (2020).
- [56] S. Finazzi and R. Parentani, Black hole lasers in Bose-Einstein condensates, *New J. Phys.* **12**, 095015 (2010).
- [57] Z. Tian, S.-Y. Chä, and U. R. Fischer, Roton entanglement in quenched dipolar Bose-Einstein condensates, *Phys. Rev. A* **97**, 063611 (2018).
- [58] P. O. Fedichev and U. R. Fischer, Gibbons-Hawking Effect in the Sonic de Sitter Space-Time of an Expanding Bose-Einstein-Condensed Gas, *Phys. Rev. Lett.* **91**, 240407 (2003).
- [59] A. Retzker, J. I. Cirac, M. B. Plenio, and B. Reznik, Methods for Detecting Acceleration Radiation in a Bose-Einstein Condensate, *Phys. Rev. Lett.* **101**, 110402 (2008).

- [60] D. Hartley, T. Bravo, D. Rätzel, R. Howl, and I. Fuentes, Analogue simulation of gravitational waves in a  $3 + 1$ -dimensional Bose-Einstein condensate, *Phys. Rev. D* **98**, 025011 (2018).
- [61] S. Datta and U. R. Fischer, Inherent nonlinearity of fluid motion and acoustic gravitational wave memory, *Phys. Rev. D* **105**, 022003 (2022).
- [62] W. G. Unruh, Dumb holes and the effects of high frequencies on black hole evaporation, [arXiv:gr-qc/9409008](https://arxiv.org/abs/gr-qc/9409008).
- [63] S. Datta and U. R. Fischer, Analogue gravitational field from nonlinear fluid dynamics, *Classical Quantum Gravity* **39**, 075018 (2022).
- [64] M. Novello, E. Bittencourt, U. Moschella, E. Goulart, J. M. Salim, and J. D. Toniato, Geometric scalar theory of gravity, *J. Cosmol. Astropart. Phys.* **06** (2013) 014.
- [65] L. D. Landau and E. M. Lifshitz, *Fluid Mechanics*, Course of Theoretical Physics (Butterworth-Heinemann, Washington, DC 1987), 2nd ed., Vol. 6.
- [66] F. Dalfovo, S. Giorgini, L. P. Pitaevskiĭ, and S. Stringari, Theory of Bose-Einstein condensation in trapped gases, *Rev. Mod. Phys.* **71**, 463 (1999).
- [67] B. Damski, Formation of shock waves in a Bose-Einstein condensate, *Phys. Rev. A* **69**, 043610 (2004).
- [68] M. Visser, Emergent rainbow spacetimes: Two pedagogical examples, in *Time and Matter 2007*, edited by M. O’Loughlin, S. Stanič, and D. Veberič (University of Nova Gorica Press, Nova Gorica, 2007), pp. 191–205.
- [69] S. Weinfurtner, P. Jain, M. Visser, and C. W. Gardiner, Cosmological particle production in emergent rainbow spacetimes, *Classical Quantum Gravity* **26**, 065012 (2009).
- [70] R. Meppelink, S. B. Koller, J. M. Vogels, P. van der Straten, E. D. van Ooijen, N. R. Heckenberg, H. Rubinsztein-Dunlop, S. A. Haine, and M. J. Davis, Observation of shock waves in a large Bose-Einstein condensate, *Phys. Rev. A* **80**, 043606 (2009).
- [71] F. Marino, C. Maitland, D. Vocke, A. Ortolan, and D. Faccio, Emergent geometries and nonlinear-wave dynamics in photon fluids, *Sci. Rep.* **6**, 23282 (2015).
- [72] W. Shen, *An Introduction to Numerical Computation* (World Scientific, Singapore, 2016).
- [73] B. Riemann, Ueber die Fortpflanzung ebener Luftwellen von endlicher Schwingungsweite, *Abh. Königlichen Gesellschaft der Wissenschaften in Göttingen* **8**, 43 (1860).
- [74] E. Kersalé, *Analytic Solutions of Partial Differential Equations* (University of Leeds, Leeds, 2004).
- [75] S. Weinberg, *Gravitation and Cosmology: Principles and Applications of the General Theory of Relativity* (Wiley, New York, 1972).
- [76] Lord Rayleigh, On the theory of long waves and bores, *Proc. R. Soc. A* **90**, 324 (1914).
- [77] G. E. Volovik, Hydraulic jump as a white hole, *Sov. JETP Lett.* **82**, 624 (2005).
- [78] G. Jannes, R. Piquet, P. Maïssa, C. Mathis, and G. Rousseaux, Experimental demonstration of the supersonic-subsonic bifurcation in the circular jump: A hydrodynamic white hole, *Phys. Rev. E* **83**, 056312 (2011).
- [79] É. Rolley, C. Guthmann, M. S. Pettersen, and C. Chevallier, The hydraulic jump in liquid helium, *AIP Conf. Proc.* **850**, 141 (2006).
- [80] G. Rousseaux and H. Kellay, Classical hydrodynamics for analogue space-times: open channel flows and thin films, *Phil. Trans. R. Soc. A* **378**, 20190233 (2020).
- [81] L.-P. Euvé, S. Robertson, N. James, A. Fabbri, and G. Rousseaux, Scattering of Co-Current Surface Waves on an Analogue Black Hole, *Phys. Rev. Lett.* **124**, 141101 (2020).
- [82] J. S. Montes and H. Chanson, Characteristics of undular hydraulic jumps: Experiments and analysis, *J. Hydraul. Eng.* **124**, 192 (1998).
- [83] J. Fourdrinoy, S. Robertson, N. James, A. Fabbri, and G. Rousseaux, Correlations on weakly time-dependent transcritical white-hole flows, *Phys. Rev. D* **105**, 085022 (2022).
- [84] R. S. Johnson, Shallow water waves on a viscous fluid—The undular bore, *Phys. Fluids* **15**, 1693 (1972).
- [85] H. Steinrück, W. Schneider, and W. Grillhofer, A multiple scales analysis of the undular hydraulic jump in turbulent open channel flow, *Fluid Dyn. Res.* **33**, 41 (2003).
- [86] A. M. Kamchatnov, *Nonlinear Periodic Waves and Their Modulations* (World Scientific, Singapore, 2000).
- [87] A. V. Gurevich and L. P. Pitaevskiĭ, Nonstationary structure of a collisionless shock wave, *Sov. Phys. JETP* **38**, 291 (1974).
- [88] G. Arfken, H. Weber, and F. Harris, *Mathematical Methods for Physicists: A Comprehensive Guide* (Elsevier Science, New York, 2013).